ISSN 1392 - 1207. MECHANIKA. 2005. Nr.4(54)

Friction torque of a rotary shaft lip type seal - a comparison between test results and finite element simulation

S. Plath*, S. Meyer, V.M. Wollesen*****

**Technische Universität Hamburg-Harburg, AB Konstruktionstechnik 1, D-21071 Hamburg, Germany, E-mail: simon.plath@tuhh.de*

***Technische Universität Hamburg-Harburg, Denicke str. 17, D-21071 Hamburg, Germany, E-mail: stefan.meyer@tuhh.de.*

****Technische Universität Hamburg-Harburg, Denicke str. 17, D-21071 Hamburg, Germany, E-mail: wollesen@tuhh.de*

1. Introduction

The Rotary Shaft Lip Type Seal (RWDR) is a machine element for the sealing of rotating unions in mechanical engineering. Even after today's state of the art, the operation of the RWDR is insufficiently avowed.

Nonlinear elastic behaviour of elastomers is characterized by time and temperature dependency. This could not be implemented sufficiently into material model, so that accurate statements of the material behaviour under different operating conditions can be made. From the fact that operating conditions in the sealing gap are not exactly known, the friction, which owns in the sealing gap, can only be described by a simple mathematical friction law. Thus sufficient life span computation of the RWDR with respect to different operating conditions is not possible.

The comparison of experimental results and Finite Element Analysis (FEA) can be used for the verification of existing material models and friction laws. The aim of that is to get a better description of the real conditions in FEA, in order to get more detailed results.

2. Theory

The RWDR is standardised in DIN 3760 [1]. Fig. 1 shows the fundamental descriptions of the RWDR.

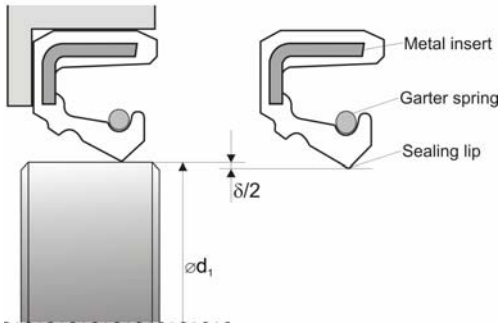

Fig. 1 RWDR with important terms

The installation of the RWDR leads to an expansion of the sealing lip, which results out of the diameter overlap δ. Due to the expansion, of the sealing lip, contact normal force is applied onto the shaft. The total radial force roughly results out of 50% tension spring component, 40% tension component of the elastomer and 10% bending component of the elastomer [2]. The radial force can be determined in static condition with a radial force measuring instrument [1]. A low value of the radial force is preferable, in order to minimize friction and wear of the seal. On the other hand the radial force must be large enough, in order to guarantee the sealing function.

The effect of those geometrical dimensions of the RWDR is typical pressing distribution (Fig. 2), which results from the contact normal force. The pressing distribution is characterized by a maximum pressing force and a high increase on the oil side and a flat decrease on the air side.

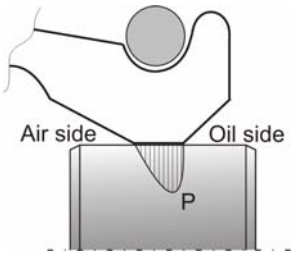

Fig. 2 Pressing distribution

For sealing function this asymmetrical pressing distribution is necessary. The pressing distribution and the friction force (resulting out of the rotating shaft) lead to characteristic shear strain of the sealing lip (Fig. 3). Different function hypotheses of seal mechanisms, which are based on pressing distribution and shear strain of the sealing lip, are listed in the literature [3].

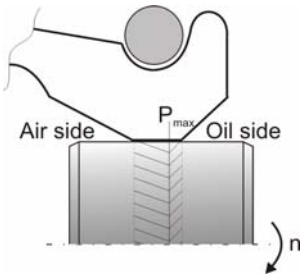

Fig. 3 Shear strain of the sealing lip

The friction in the sealing zone is characterized by the tribological system, which consists out of the RWDR, the fluid and the shaft (Fig. 4).

For the FEA a pure elastomer/metal friction is preconditioned. The existence of fluid in the sealing zone is neglected, in order to be able to implement a simple friction law into the FEA.

The friction of both friction partners (elastomer, metal) cannot be described by the Coulomb friction law [4,5].

$$F_R = \mu F_N \quad (1)$$

where F_R is friction force; μ is coefficient of friction; F_N is contact normal force.

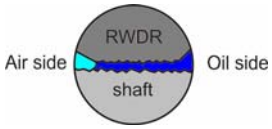

Influencing variables of the tribological System		
RWDR - Shaft	Fluid	Operation condition
- material - geometry - surface roughness - etc.	- viscosity - additive - etc.	- rotation speed - temperature - pressure - vibrations - etc.

Fig. 4 Tribological System: RWDR - fluid – shaft

The friction of an elastomer is characterized by
- contact normal force;
- temperature;
- sliding velocity (rotation speed).

At present a friction law is being developed to get a better description of the conditions in the sealing gap, containing the contact normal force, the temperature and the rotation speed. So far the FEA is accomplished exemplarily with the Coulomb friction law.

3. Test rig and results

Today friction torque can be determined metrologically exactly. For this an aerostatic bearing of the RWDR is used. A draft for friction torque test rig is shown in Fig. 5.

The RWDR is mounted in a vertical test cell. The housing where the RWDR is installed, is bedded by an air bearing (aerostatic, frictionless). The air bearing will ensure, that only the friction with the strain gauge (DMS) arising in the sealing contact area is measured. The measured frictional force of the DMS can be converted - using geometrical dimensions - into existing friction torque.

By changing rotation speed, friction behaviour can be examined at different rotation speeds. Resulting out of the given shaft diameter and the different rotation speed is a sliding speed between shaft and RWDR of 2-8 m/s.

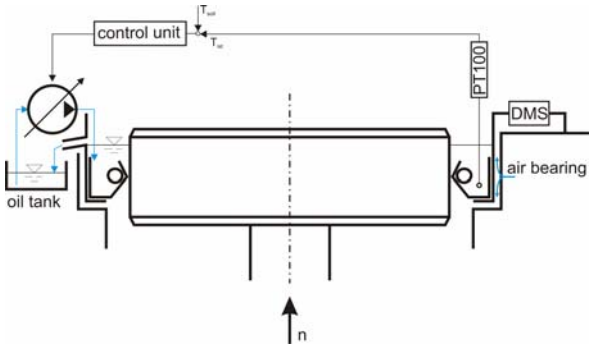

Fig. 5 Friction torque test rig

A further possibility to analyze the friction behaviour offers temperature control. The oil temperature is measured with a thermal element and can be kept at constant level by temperature control unit. Hence friction torque analysis at different levels of temperature can be performed.

The intention of those friction torque trials is, to receive a dependency of friction moment on different operating parameters. By the experimental setup the following variations are possible:
- different relative velocity (rotation speed 2-8 m/s);
- change of temperature (oil temperature: 50-100 °C);
- radial force (short the spring).

The Table 1 shows the test plan set-up, which is executed with different RWDR, in order to receive statistic confidence level for the measurement results. In addition, the analysis with increased radial force is accomplished, that is based on the same cycle.

Table 1

Test plan

Temperature, °C	500 1/min	1000 1/min	1500 1/min	2000 1/min
50	x	x	x	x
60	x	x	x	x
70		x	x	x
80		x	x	x
90			x	x
100			x	x
RWDR A 80x100x10 DIN3760, NBR				

The focus of that investigation is the temperature variation and the rotation speed. The RWDR is examined in a rotation speed interval from 500 to 2000 1/min with a gradation of 500 1/min. Here the temperature range varies in 10°C steps, regarding the spectrum from 50 to 100°C.

Measurement results showed, that with a rotation speed of 500 1/min (1000 1/min) a temperature of 70°C (90°C) was not reached. As a result of the selected measuring point locations, each RWDR can be measured at 18 different operating points.

4. Test evaluation

In Fig. 6, a complete analysis cycle of a standard RWDR is represented. The analysis results are shown in dependence on friction torque over the rotation speed. Each point in the diagram represents a static operating point, as indicated in Table 1. For a clearly laid out illustration, points of the same temperature are connected by a line.

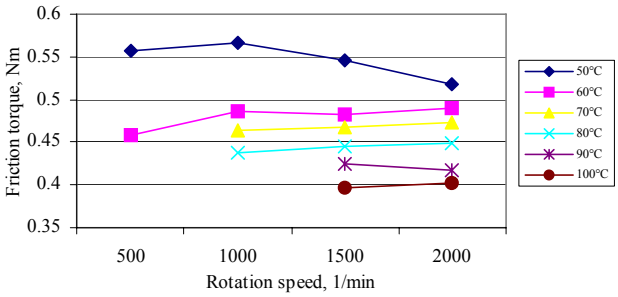

Fig. 6 RWDR, normal radial force

As graphically illustrated in Fig. 6, a dependence of the friction moment on temperature can be seen. At con-

stant rotation speed the friction moment will decrease with a rising temperature.

This behaviour is based on the material properties of the elastomer. The acting spring force generally will not be influenced in this existing temperature spectrum from 50 to 100°C. The elastomer tension and bending property decreases with rising temperature. Hence the radial pressing decreases and as a result of that the friction moment drops.

To clearly highlight the dependence of friction moment on rotation speed, the measurements results are demonstrated in Fig. 7. Here friction torque is represented over the temperature, whereby operating points of the same rotation speed are connected.

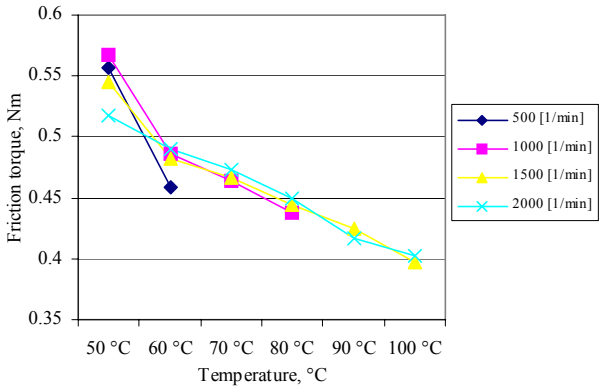

Fig. 7 RWDR, normal radial force

Fig. 7 shows, that operating points of the same temperature have similar friction torque values. The distribution of the friction torque values is with 50 and 60°C under 5 per cent, and within other temperatures with approx. 2 per cent. An accurate prediction over the friction torque at different rotation speeds is not possible due to these small distributions.

In addition Fig. 7 clarifies the temperature dependence of the friction torque. With an increase of the temperature from 60 to 100°C the friction torque decreases approximately linear.

The further parameter is the initial stress in the spring. By shortening the spring, an increase of radial pressing will be reached and so the friction torque in dependence of the radial force can be examined.

The results of a test trial with shortened spring are displayed in Fig. 8 and Fig. 9.

Friction torque level of the RWDR with a short

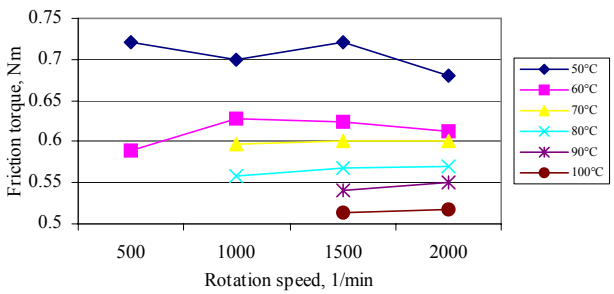

Fig. 8 RWDR, high radial force

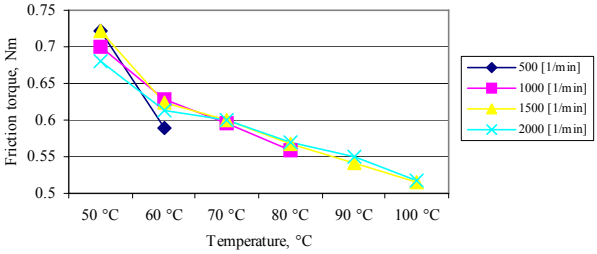

Fig. 9 RWDR, high radial force

spring is higher than with a normal spring. Resulting out of those test trials it can be seen, that the friction torque increases with a high radial pressing. The temperature dependence of the friction toque is to be recognized again.

5. Finite Element Analysis (FEA) with MSC.Marc/Mentat

An intention of the FEA is to make a comparison between the results of the friction torque measurements and the FE-results. The accomplished friction torque measurements describe the substantial boundary conditions for the FE-modelling. The FE-modelling is based on mechanical analysis.

Basis of the FE-modelling gives a micro copied RWDR, which is the basic geometry for FE-mesh (Fig. 10).

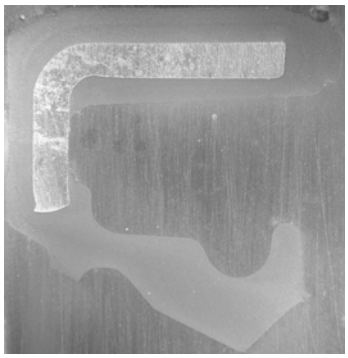

Fig. 10: Micros copied RWDR

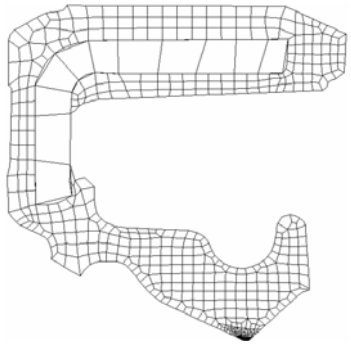

Fig. 11 FE-mesh

Due to axial symmetrical characteristics of the RWDR shaft system a modelling with 2D description is accomplished. The refinement of the mesh is to be recognized in Fig. 11. The element size is in the range of the sealing zone with an edge length of 2 µm. Fine cross linking within the range of the sealing lip allows accurate

modelling of the friction.

The boundary conditions are clarified in Fig. 12. The outside diameter of the RWDR is modelled with a fixed bearing. The spring is retained by a rigid body, which point load affects. The spring action working in reality is converted into the equivalent point load.

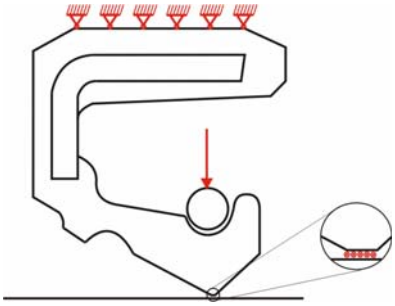

Fig. 12 Boundary conditions

The friction is modelled exemplarily by a Coulomb friction model. Temperature and rotation speed are not considered in the FE-model. Coefficient of friction of μ=0.35 is accepted, in order to get comparable friction torque values with the measured friction attempts.

In Table 2 the basis material properties are represented.

Table 2

Material property

Component part	Real material property	FEA material
Shaft	linear elastic	isotropic E-Modul: 210GPa Poisson ratio: 0.3
RWDR Metal insert		
RWDR Elastomer	non-linear hyper-elastic*	Mooney Rivlin C01 = 0.789757 C10 = 0.164362
Garter spring	linear elastic	rigid body with point-load

*The acceptance of the material behaviour as hyper-elastic is a simplification, since momentarily only an uni-axial traction test of the elastomer is presented. Hence the visco-elastic material behaviour of elastomers cannot be considered. To the material behaviour of elastomers refers the work of [6].

6. FEA results

The results of FEA are represented in Fig. 13 and Fig. 14. It represents the equivalent stress of Von-Mises.

A higher stress is recognized in the sealing due to a higher radial force (Fig.13 and Fig. 14). With the increased radial force the friction torque rises in the FEA. Measurement results show, that the friction torque increases with a rising radial force. A comparison of FE results and test results is possible. An accurate statement is however not possible with the mentioned simplifications. The consideration of temperature and the number of revolutions will lead to more exact results.

Pressing distribution of the radial force is comparable in Fig. 15 similarly to the theoretical pressing distribution in Fig. 2. The figure shows typical asymmetrical pressing distribution.

Moreover the distortion of the elastomer in Fig. 16 is comparable to Fig. 3.

Respecting the mentioned simplifications (material model, friction) a comparison of the results is in principle possible. Following the increase of the radial force in the attempt and in the FEA leads to an increased friction torque.

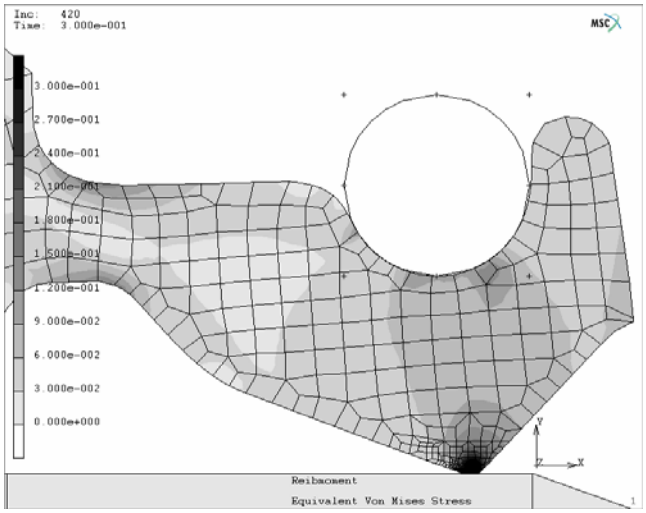

Fig. 13 Equivalent Von-Mises stress - normal radial force- friction torque = 0.48 Nm

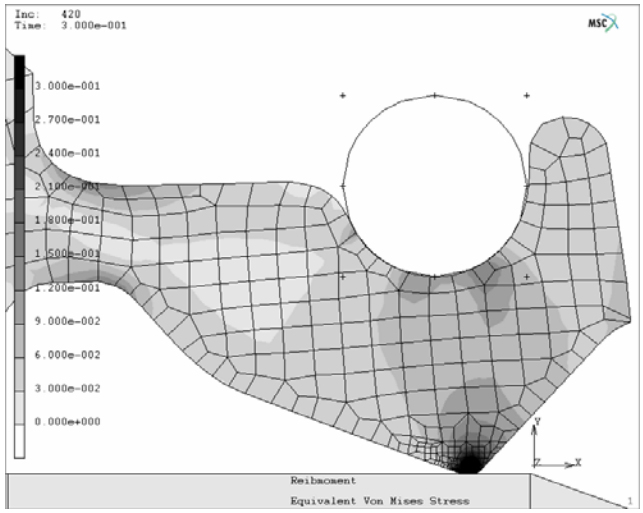

Fig. 14 Equivalent Von-Mises stress - high radial force - friction torque = 0.52 Nm

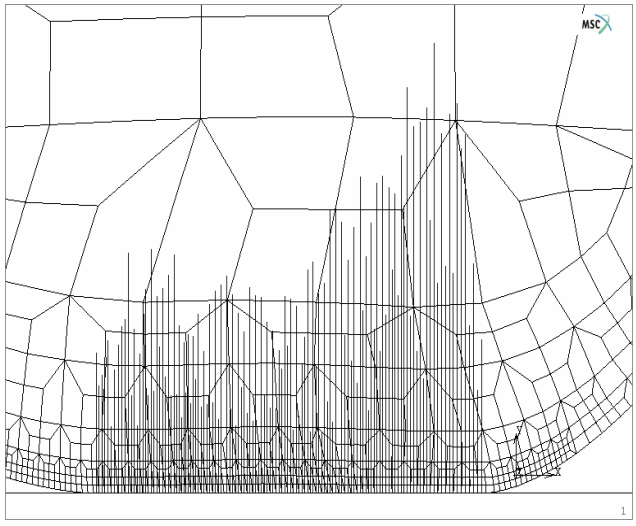

Fig. 15 Pressing distribution

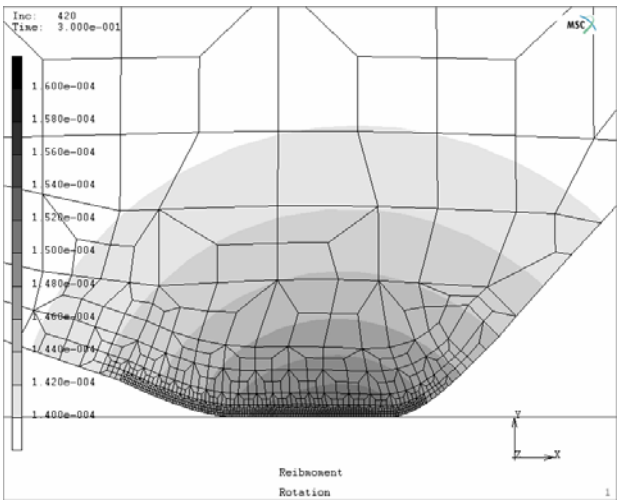

Fig. 16 Shear strain

7. Conclusions

The comparison shows additionally the momentary simplifications of the FEA. The coefficient of friction μ, which has been assumed as constant, has to be replaced by a friction function in the FEA. Here a coupled thermomechanical analysis is necessary, in order to be able to consider temperature into the friction function. Moreover a change of the hyper-elastic to the visco-elastic material behaviour is meaningful, to respect the material behaviour of the elastomer. Within the working level area this existing FE-model will be updated and modified with the mentioned items.

References

1. Deutsches Institut für Normung (DIN): DIN 3760 – Radialwellendichtringe. Berlin, Beuth Verlag, 1993.
2. N.N.: Simrit-Katalog. Freudenberg Dichtungs- und Schwingungstechnik KG, 1996.
3. **Müller H.K.** Abdichtung bewegter Maschinenteile. Waiblingen, Medienverlag, 1990.
4. **Freitag E., Happ B.** Zur Geschwindigkeits-, Temperatur- und Druckabhängigkeit der Adhäsionsreibung von NBR-Gummiwerkstoffen. Schmierungstechnik 21, 1990, Nr.7, s.199-202.
5. **Hauk S., Freitag E., Hornberger K.** Reibmodelle für elastomere und thermoplastische Werkstoffe und ihre Implementierung in Finite-Elemente-Codes. Materialwissenschaft und Werkstofftechnik 28, 1997, Nr.12, s.561-566.
6. **Gohl W., Spies K.H.** Elastomere – Dicht- und Konstruktionswerkstoff. Reiningen, expert-Verlag, 2003.

S. Plath, S. Meyer, V.M.Wollesen

RADIALINIO SANDARINIMO ŽIEDO TRINTIES MOMENTAS: BANDYMŲ IR MODELIAVIMO BAIGTINIŲ ELEMENTŲ REZULTATŲ PALYGINIMAS

R e z i u m ė

Radialinio sandarinimo žiedo ilgaamžiškumui esminę įtaką turi trinties momentas, kuris priklauso nuo darbo sąlygų ir gali būti išmatuojamas. Trinties momento skaičiavimas baigtinių elementų analizės (BEA) metodu leidžia minimizuoti bandymų išlaidas. Radialinio sandarinimo žiedo BEA galima atlikti tik darant didelius supaprastinimus. To priežastis − teorinių žinių apie sandarinimo mechanizmą stoka. Čia aprašomi tyrimai yra riebokšlio BEA pavyzdys. Be to, pateikiamas eksperimentų ir BEA rezultatų palyginimas.

S. Plath, S. Meyer, V.M. Wollesen

FRICTION TORQUE OF A ROTARY SHAFT LIP TYPE SEAL - A COMPARISON BETWEEN TEST RESULTS AND FINITE ELEMENT SIMULATION

S u m m a r y

The life span of a Rotary Shaft Lip Type Seal (RWDR) depends substantially on the friction torque. The friction torque can be determined metrological exactly and it depends on different operating conditions. Calculation of the friction moment with the Finite Element Analysis (FEA) allows the minimization of cost-intensive tests. At present FEA of the RWDR is possible only with significant simplifications. A reason for this is that the sealing mechanism is insufficiently described by the theory. This research shows exemplarily the FEA of the friction torque of the RWDR. Furthermore a comparison of the FE-results and test results is shown.

С. Платх, С. Мэер, В.М. Воллесен

МОМЕНТ ТРЕНИЯ РАДИАЛЬНОГО УПЛОТНИТЕЛЬНОГО КОЛЬЦА – СОПОСТАВЛЕНИЕ РЕЗУЛЬТАТОВ ЭКСПЕРИМЕНТОВ И МОДЕЛИРОВАНИЯ МЕТОДОМ КОНЕЧНЫХ ЭЛЕМЕНТОВ

Р е з ю м е

Долговечность радиального уплотнительного кольца (РУК) в основном зависит от момента трения. Момент трения зависит от рабочих условий и может быть определен измерением. Подсчет момента трения методом конечных элементов (МКЭ) уменьшает затраты при экспериментальных исследованиях. Моделирование МКЭ РУК возможено лишь принимая значительные упрощения. Причиной этого является недостаточные теоретические знания механизма уплотнения. В данной работе приведен образец МКЭ уплотнительного кольца. Также дано сопоставление результатов полученных МКЭ с результатами эксперимента.

Received February 15, 2005